

# Influence of Mn Doping on the Electronic Structure and Absorption Spectrum of $\text{Ca}_2\text{SiO}_4:\text{Eu}^{2+}$ Phosphor

Chen Haitao<sup>1,2</sup>, Huang Xuefei<sup>1</sup>, Huang Weigang<sup>1</sup>

<sup>1</sup> Sichuan University, Chengdu 610064, China; <sup>2</sup> Chengdu Normal University, Chengdu 611130, China

**Abstract:** The influence of Mn doping on the  $\text{Ca}_2\text{SiO}_4:\text{Eu}^{2+}$  phosphors was investigated by the first principle calculation. Comparing with the  $\text{Ca}_2\text{SiO}_4:\text{Eu}^{2+}$  phosphor, it is found that red-shift of the absorption spectrum for the Mn-doped  $\text{Ca}_2\text{SiO}_4:\text{Eu}^{2+}$  phosphor takes place.  $\text{Mn}^{2+}$  ions substitution on  $\text{Ca}^{2+}$  sites causes an increase of the crystal field strength, which results in  $\text{Eu}5d$  level moving downward in energy. Besides,  $\text{Mn}3d$  partly enters into the top of the conduction band and the bottom of the valence band. These two reasons bring about narrow band gap and red shift of absorption spectrum.

**Key words:** silicate phosphor; light emitting diodes (LEDs); first principle calculation

It is known that divalent europiums are more stable in alkaline earth silicate hosts and more easily diffuse into the lattice sites as the ion radii of them are similar to each other<sup>[1,2]</sup>. Therefore, alkaline earth silicon compounds doped with divalent europium ions are good candidates for abundant color representation and high efficient luminescence phosphors. Particularly,  $\text{Eu}^{2+}$ -doped  $\text{Ca}_2\text{SiO}_4$  phosphors have been regarded as a kind of green emitting material for white LED with a possibility to replace sulfide based green phosphors<sup>[3]</sup>. It has been found recently that the  $\text{Eu}^{2+}/\text{Mn}^{2+}$ -codoped phosphors exhibited red emission from the  $\text{Mn}^{2+}$  ions in addition to green emission from the  $\text{Eu}^{2+}$  ions. Thus, the spectra consist of the relatively broad green and the red emission bands, which lead to a warm-white color<sup>[4-8]</sup>. What is interesting is how  $\text{Mn}^{2+}$  influences the electronic structure of  $\text{Ca}_2\text{SiO}_4:\text{Eu}^{2+}$  and improves its photo-luminescence properties. Nowadays, the first-principles method has become a valuable tool for the investigation of the electronic structures of materials<sup>[9-12]</sup>. In this paper, we have investigated the electronic structure of Mn-doped and un-doped  $\text{Ca}_2\text{SiO}_4:\text{Eu}^{2+}$  by the first-principle calculation. Atomic and bond populations, total density of states (TDOS) and partial density of states (PDOS) as well as absorption spectra of these phosphors

are computed and compared. After that, the influence of Mn doping on the electronic properties and the absorption properties of  $\text{Ca}_2\text{SiO}_4:\text{Eu}^{2+}$  is derived.

## 1 Theoretical Simulation

The calculations were performed based on the first-principle within the Cambridge Serial Total Energy Package (CASTEP) plane wave code<sup>[13]</sup>. In order to achieve accurate electronic structures, the method of total-energy functional (LDA+U) was adopted to overcome the shortcoming of LDA. Meanwhile, ultrasoft pseudopotentials were used to describe the interaction of ionic core and valence electrons. And Brillouin-zone integrations were performed using Monkhorst and Pack k-point meshes<sup>[14]</sup>. When the calculation is operated, the 500 eV for cutoff energies and  $3\times 2\times 2$  for the numbers of k-point can ensure the convergence for the total energy. When the maximum force on the atom was below  $0.003\text{ eV}\cdot\text{nm}^{-1}$ , maximum stress was below 0.05 GPa, and the maximum displacement between cycles was below 0.0001 nm. All the calculations were considered converged. Though both  $\beta$  and  $\gamma$  phases of pure  $\text{Ca}_2\text{SiO}_4$  crystallite are stable at room-temperature, only  $\beta$  phase is stable in the case of  $\text{Eu}^{2+}$ -doped  $\text{Ca}_2\text{SiO}_4$  phosphor<sup>[15]</sup>. The  $\beta$  phase of  $\text{Ca}_2\text{SiO}_4$  crystal has a trigonal structure with

Received date: March 20, 2017

Foundation item: National Science Foundation of China (51401135); Chengdu Normal University Foundation (YJRC2015-1)

Corresponding author: Huang Weigang, Ph. D., Professor, College of Material Science and Engineering, Sichuan University, Chengdu 610064, P. R. China, E-mail: huangwg56@163.com

Copyright © 2018, Northwest Institute for Nonferrous Metal Research. Published by Elsevier BV. All rights reserved.

space group P21/n. The Ca ions have two different sites: one is coordinated with seven O atoms and the other is connected with eight O atoms. Thus, it is generally accepted that the Eu atoms occupy both two Ca sites in the lattice<sup>[16]</sup>. In order to demonstrate the effect of Mn doping on the  $\text{Ca}_{2-0.04}\text{SiO}_4:0.04\text{Eu}^{2+}$  phosphor, super-cells containing 84 atoms of  $\text{Ca}_{2-0.08}\text{SiO}_4:0.04\text{Eu}^{2+}0.04\text{Mn}^{2+}$  are formed (Fig.1).

## 2 Results and Discussion

### 2.1 Atomic charges population

The Mulliken atomic charges populations of  $\text{Ca}_2\text{SiO}_4:\text{Eu}^{2+}$  are shown in Table 1. It is easily seen that O ions own negative charge because of obtaining electrons, while Ca and Eu ions own positive charges due to losing electrons. Covalent bonds are localized between Si atoms and O atoms because Si atoms possess relatively weak ability to lose electrons. Ca and Eu atoms form ionic bonds with O atoms as Ca and Eu atoms possess the strong ability to lose electrons. On the other hand, it is  $\text{Eu}^{2+}$  not  $\text{Eu}^{3+}$  replacing one  $\text{Ca}^{2+}$  of  $\text{Ca}_{24}\text{Si}_{12}\text{O}_{48}$  because seven electrons

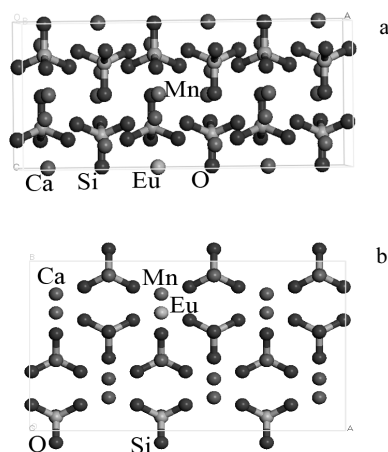


Fig.1 Top view (a) and side view (b) of the structure of super-cells of  $\text{Ca}_2\text{SiO}_4:\text{Eu}^{2+}$  with substitution of Mn atoms for Ca atom

are localized in the 4f orbital of Eu ion in  $\text{Ca}_{23}\text{EuSi}_{12}\text{O}_{48}$ . It is also seen from Table 1 that  $\text{Mn}^{2+}$  indeed displaces one  $\text{Ca}^{2+}$  of  $\text{Ca}_{24}\text{Si}_{12}\text{O}_{48}$ .

### 2.2 Band structures

Fig.2 plots the band structures of Mn-doped and un-doped  $\text{Ca}_2\text{SiO}_4:\text{Eu}^{2+}$  for the case 1 in Table 1, where the TDOS is also plotted. It is found that each of these two phosphors shows a direct optical band gap, which makes the transition probability higher than that of the indirect band gap, so it can enhance luminescence property<sup>[17]</sup>. The valence band maximum (0 eV) and conduction band minimum (4.71 eV) at the G point of Brillouin zone in Fig.2a.

Thus, the calculated band gap energy is 4.71 eV. When Mn atoms are doped, the calculated band gap energy is 4.33 eV, which is much smaller than the case of Mn-undoped. The reason is that the partial substitution of Mn atoms for Ca atoms results in higher valence band and smaller band gap width. Besides, the labels of the energy bands (1, 2, 3, 4, 5 and 6) and the interband transitions (a, b and c) obtained from the analysis of Fig. 4 are shown in Fig.2.

Fig.3 shows the calculated band structures and the density of states of Mn-doped and un-doped  $\text{Ca}_2\text{SiO}_4:\text{Eu}^{2+}$  for the case of 2 in Table 1. Similar to the case 1, direct optical band gaps appear in the case 2. It is seen that the valence band maximum and conduction band minimum are located at 0 and 4.71 eV in Fig.3a, respectively. Therefore, the calculated band gap energy is 4.71 eV. As one Ca atom is substituted by one Mn atom, its band gap energy is small to 4.24 eV. Therefore, the doping of Mn atoms elevates the valence band maximum and narrowing the band gap. In addition, the labels of the energy bands (7, 8, 9, 10, 11 and 12) and the interband transitions (d, e and f) are obtained from the analysis of Fig.5.

### 2.3 Densities of states

Fig.4 shows the atom-resolved partial density of state (PDOS) for Mn-doped and un-doped  $\text{Ca}_2\text{SiO}_4:\text{Eu}^{2+}$  for the case 1. Only the top of the valence band and the bottom

Table 1 Atomic charges population of  $\text{Ca}_2\text{SiO}_4:\text{Eu}^{2+}$  phosphors

Case	$\text{Ca}_{23}\text{EuSi}_{12}\text{O}_{48}$						$\text{Ca}_{22}\text{EuMnSi}_{12}\text{O}_{48}$					
	Atom	s	p	d	f	Total	Atom	s	p	d	f	Total
1	O	1.88	5.31	0	0	7.19	O	1.86	5.22	0	0	7.08
	Si	0.68	1.50	0	0	2.18	Si	0.70	1.47	0	0	2.16
	Ca	2.18	6.00	0.34	0	8.52	Ca	2.14	6	0.6	0	8.74
	Eu	2.17	6.24	0.67	7	16.07	Eu	2.14	6.08	0.59	7	15.82
							Mn	0.3	0.47	5.22	0	6
2	O	1.86	5.23	0	0	7.09	O	1.86	5.22	0	0	7.08
	Si	0.70	1.47	0	0	2.17	Si	0.69	1.46	0	0	2.15
	Ca	2.14	6.00	0.60	0	8.74	Ca	2.14	6	0.6	0	8.74
	Eu	2.14	6.13	0.60	7	15.87	Eu	2.17	6.19	0.58	7	15.95
							Mn	0.33	0.46	5.24	0	6.03

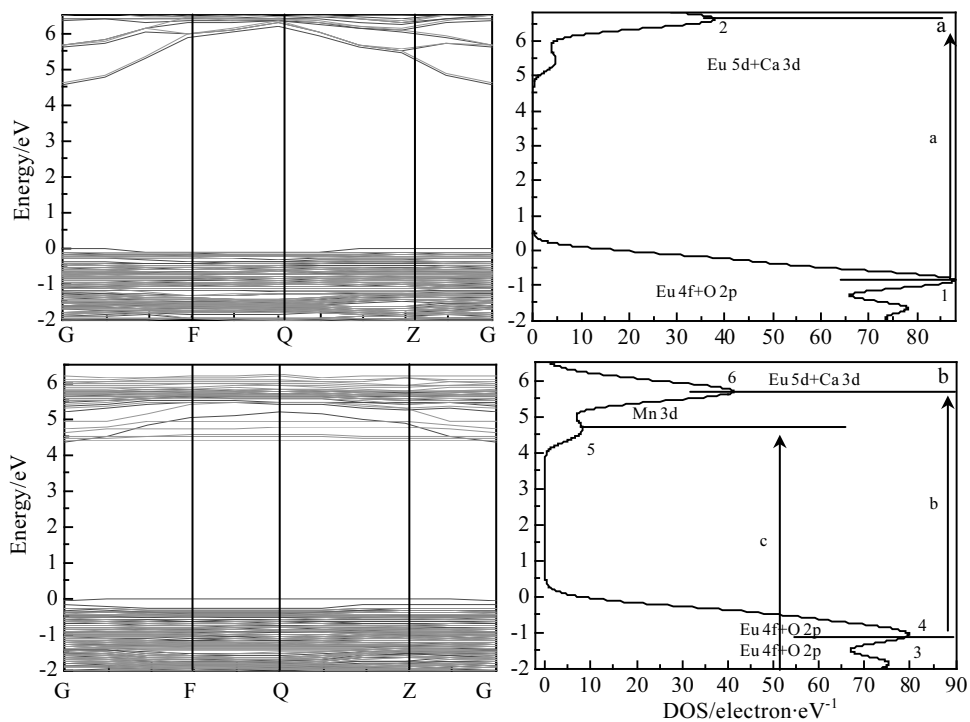


Fig.2 Band structure and total density of state (DOS) of  $\text{Ca}_2\text{SiO}_4:\text{Eu}^{2+}$  without (a) and with (b) substitution of one Mn atom for Ca atom for the case 1 in Table 1

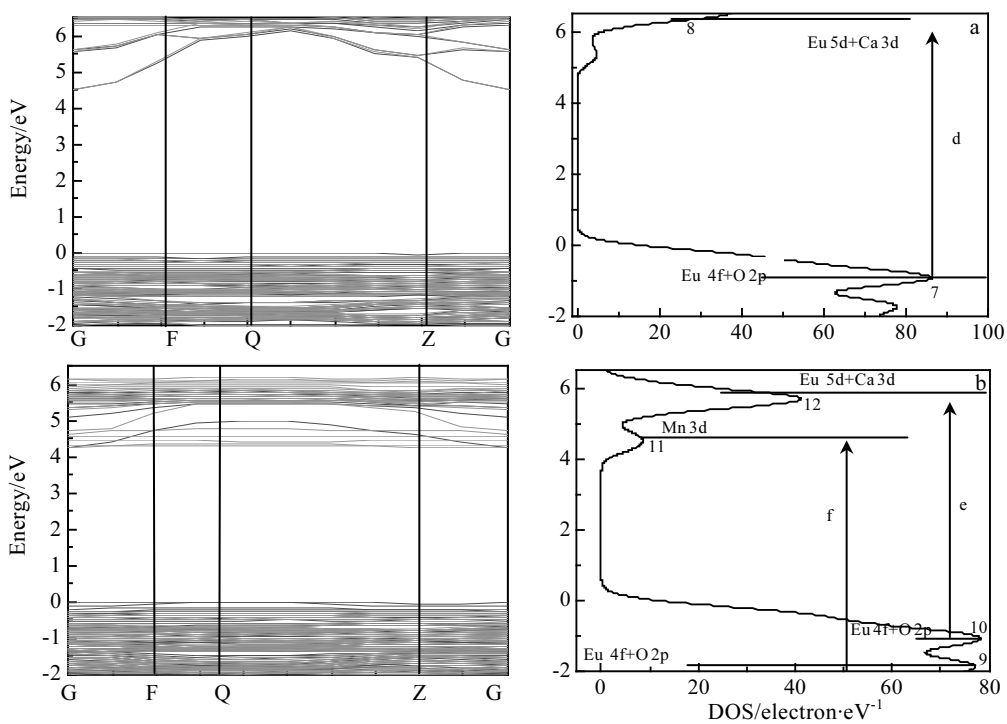


Fig.3 DOS of  $\text{Ca}_2\text{SiO}_4:\text{Eu}^{2+}$  without (a) and with (b) substitution of Mn atom for Ca atom for the case 2 in Table 1

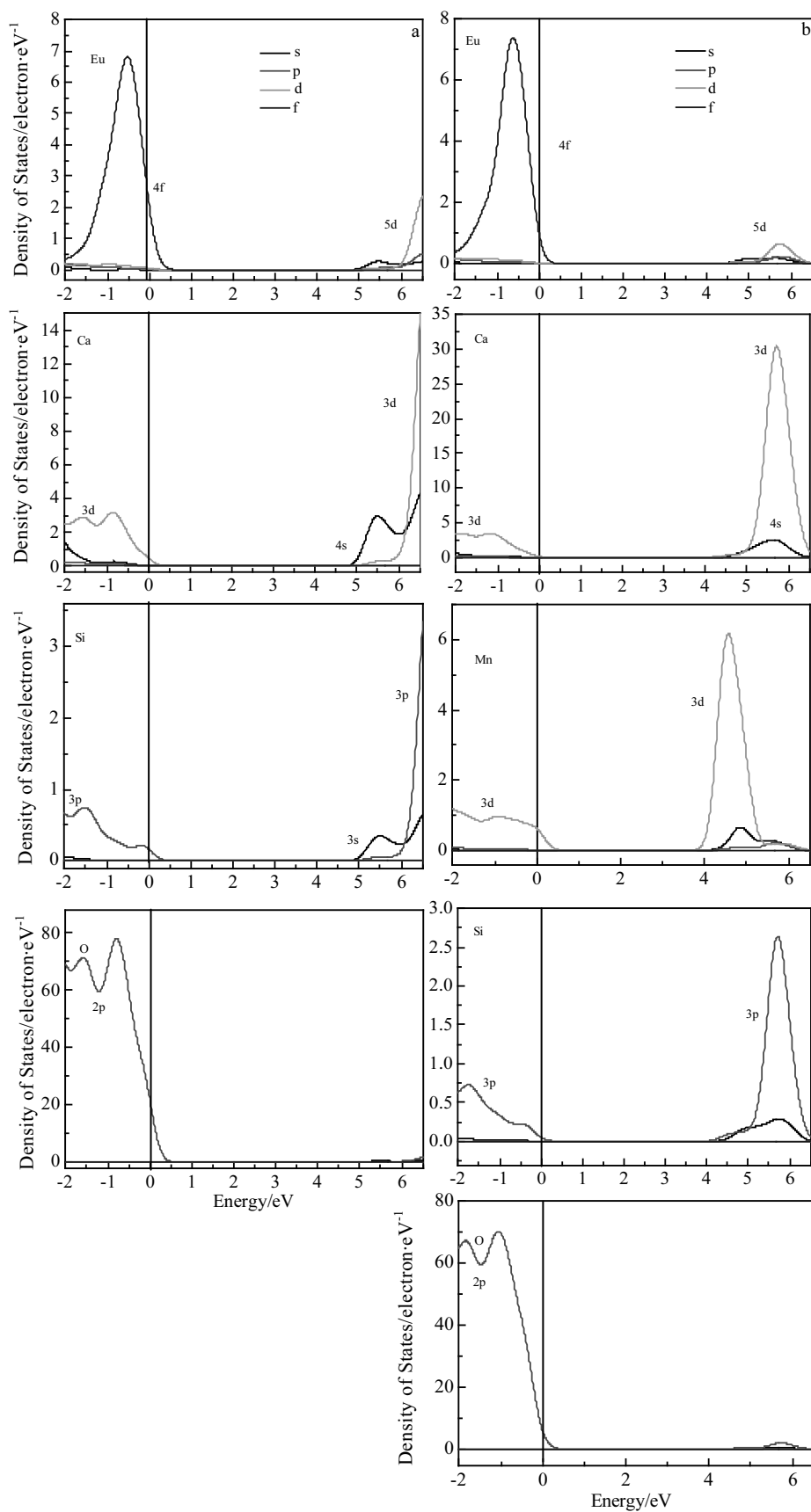


Fig.4 PDOS of  $\text{Ca}_2\text{SiO}_4: \text{Eu}^{2+}$  without (a) and with (b) substitution of one Mn atom for Ca atom for the case 1 in Table 1

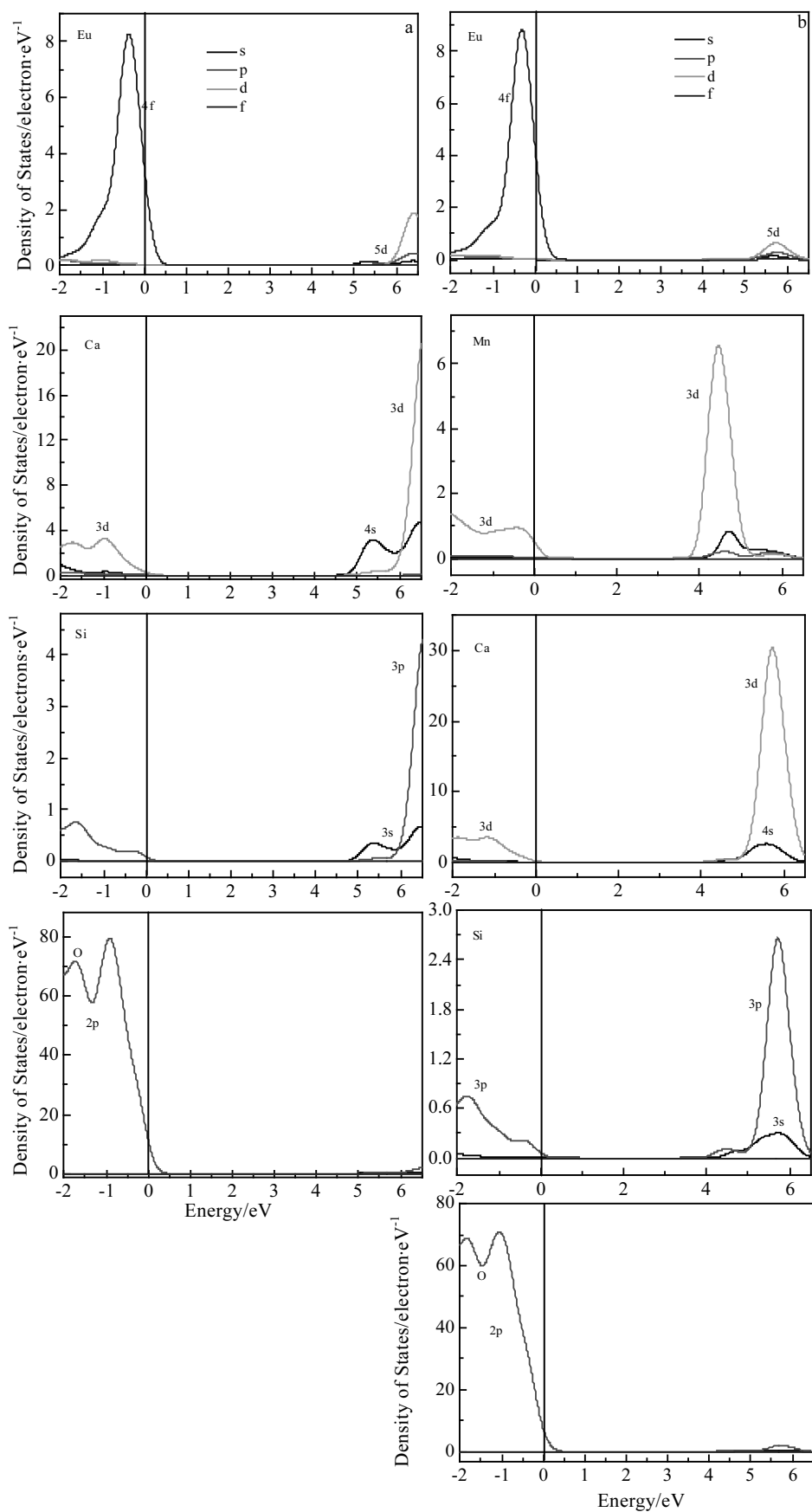


Fig. 5 PDOS of  $\text{Ca}_2\text{SiO}_4:\text{Eu}^{2+}$  without (a) and with (b) substitution of one Mn atom for Ca atom for the case 2 in Table 1

of the conduction band are shown as the optical absorption is mainly determined by the states close to the band gap. In order to display clearly, the Fermi level is set to zero. The bottom of the conduction band mainly stems from the hybridized orbits Ca3d, Mn 3d and Eu5d, while the top of the valence band is mainly composed of the O 2p orbital, partly derived from Eu4f. It can be seen from Fig. 4a that the band 1 with maximum at  $-1.22$  eV in Fig. 2a mainly originates from O2p state, and band 2 with maximum at  $4.44$  eV mainly stems from Ca4s state, while the band 3 with maximum at  $6.22$  eV is mainly contributed by Ca3d and Eu5d states. When Mn atom is doped, the band 4 with maximum at  $-1.84$  eV mainly originates from O2p and Eu 4f states, band 5 with maximum at  $-1.04$  eV is also mainly composed of O2p and Eu4f states, band 6 with maximum at  $4.66$  eV mainly originates from Mn 3d state, while band 7 with maximum at  $5.72$  eV mainly originates from Ca 3d and Eu 5d states. It is seen from Fig. 4b that Mn 3d, Eu 5d and Ca3d orbits overlap each other, which results in the energy electron transition from Mn3d and Ca 3d to the empty band of Eu 5d states. The Mn 3d splits and partly enters into the top of the conduction band and the bottom of the valence band due to the  $\text{Eu}^{2+}$ . Thus, the band gap energy of the Mn-doped  $\text{Ca}_2\text{SiO}_4:\text{Eu}^{2+}$  is much smaller than that of Mn-undoped.

The PDOS of Mn-doped and un-doped  $\text{Ca}_2\text{SiO}_4:\text{Eu}^{2+}$  for the case 2 is shown in Fig. 5. It can be seen from PDOP in Fig. 5a that the bottom of the conduction band mainly stems from Ca3d and Eu5d states, and the top of the valence band is mainly composed of the O2p, Eu4f and Ca3d states, which is similar to the case of Ca(1) in Fig. 4a. The band 8 with maximum at  $-0.96$  eV mainly originates from O2p state, and band 9 with maximum at  $5.79$  eV is mainly contributed by Ca 3d, Si 2p and Eu 5d states. When one Mn atom is co-doped, the bottom of the conduction band mainly stems from Ca 3d, Mn3d and Eu 5d states, and the top of the valence band is mainly composed of O2p, Eu4f, Ca3d and Mn 3d states, which is similar to the case 1 in Fig. 4b. Furthermore, the band 10 with maximum at  $-1.85$  eV mainly originates from O2p and Ca3d and Mn3d states, band 11 with maximum at  $-1.06$  eV is mainly composed of O2p, Ca 3d, Mn3d and Eu4f states, and band 12 with maximum at  $4.52$  eV mainly stems from Mn3d states, while band 13 with maximum at  $5.72$  eV is mainly contributed by Ca3d and Eu 5d states. It is seen from Fig. 5b that Mn 3d, Ca3d and Eu 5d orbits overlap each other, which results in the conduction band charge transfer of the electrons from Mn 3d, Ca3d to the empty band of and Eu5d states. Besides, it is seen from Figs. 4b, and 5b that the overlap between Mn3d and Eu4f, 4d states leads to the effective resonance-type energy transfer from  $\text{Eu}^{2+}$  to  $\text{Mn}^{2+}$ , which is in agreement with the results from Ref. [4-8].

## 2.4 Absorption spectra

The optical absorption coefficient of materials is determined by the quantum mechanical transition rate which is expressed as <sup>[18]</sup>:

$$W_{i \rightarrow f} = \frac{4\pi^2}{h} |M|^2 g(h\nu) \quad (1)$$

where  $W_{i \rightarrow f}$  is transition rate for exciting an electron in an initial state  $\varphi_i$  to a final state  $\varphi_f$  by absorption of a photon with frequency  $\nu$ ,  $M$  is the matrix element, and  $g(h\nu)$  is the joint density of states. The  $|M|^2$  is usually regarded as a constant for a direct optical transition, so that the luminescence intensity is only determined by the joint density of states  $g(h\nu)$ . As shown in Fig. 2, the initial state can be considered as a constant in the transition process as the lower band is very flat, so the  $g(h\nu)$  is proportional to the final state  $\varphi_f$ . Therefore, the transition, the optical absorption coefficient and the emission intensity are proportional to the density of the upper states.

By comparing the total DOS in Fig. 4 and absorption spectra in Fig. 6, it is found that the phosphor without Mn atom (black curve) displays several broad absorption peaks, such as absorption peak  $\alpha$  at  $7$  eV ( i. e.,  $177$  nm) which is readily assigned to transition a. When Mn atom is doped, the absorption peak  $\beta$  at  $6.8$  eV ( i. e.,  $180$  nm) is mainly corresponding to the inter-band transitions b and c. As shown in Fig. 4a, the density of the upper states is mainly contributed by the Eu and Ca atoms for  $\text{Ca}_2\text{SiO}_4:\text{Eu}^{2+}$ , while the upper states are determined by the combined contributions of the Ca, Mn and Eu atoms for Mn-doped  $\text{Ca}_2\text{SiO}_4:\text{Eu}^{2+}$ . When Mn atoms are doped, a red-shift of absorption spectrum takes place, which is in agreement with the results of the  $\text{Ca}_{5-0.01}\text{Mg}_{1-0.1}\text{Si}_3\text{O}_{12}:0.01\text{Eu}^{2+}, 0.1\text{Mn}^{2+}$  in Ref.[4]. The reason is that the Eu5d level moves downward in energy; meanwhile, Mn3d splits and partly enters into the top of the conduction band and the bottom of the valence band.

Fig. 7 plots the absorption spectra Mn-doped and un-doped  $\text{Ca}_2\text{SiO}_4:\text{Eu}^{2+}$  for the case 2. Comparing the total DOS of  $\text{Ca}_2\text{SiO}_4:\text{Eu}^{2+}$  in Fig. 5a and its absorption spectra of the phosphor without Mn atom (black curve) in Fig. 7, it is seen

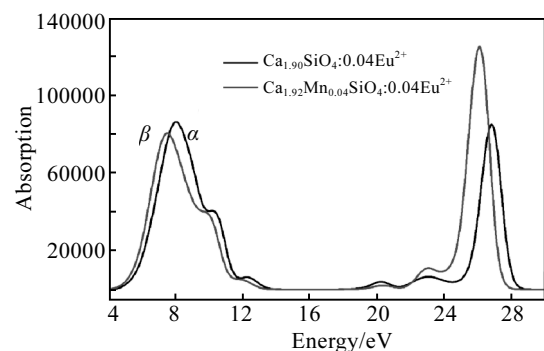


Fig. 6 Absorption spectra of  $\text{Ca}_2\text{SiO}_4:\text{Eu}^{2+}$  without and with substitution of Mn atom for Ca atoms for the case 1 in Table 1

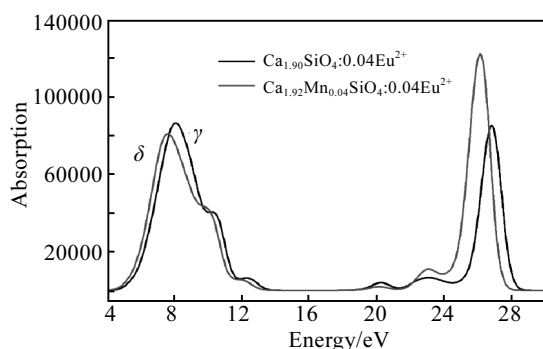


Fig. 7 Absorption spectra of  $\text{Ca}_2\text{SiO}_4:\text{Eu}^{2+}$  without and with substitution of Mn atom for Ca atom for the case 2 in Table 1

that the absorption peak  $\gamma$  at 8 eV (i. e., 155 nm) is mainly corresponding to the transition process d. As Mn atom is doped, the absorption peak  $\delta$  at 6.8 eV (i. e., 178 nm) is most readily assigned to transition e and f. Being similar to the case 1, red-shift of absorption spectrum is attributed to the magnitude of d-orbital splitting of the  $\text{Eu}^{2+}$  ions and the Eu 5d level moving downward.

### 3 Conclusions

In order to explore the influence of Mn doping on the  $\text{Ca}_2\text{SiO}_4:\text{Eu}^{2+}$  phosphor, the electronic structure and absorption spectra of Mn-doped and un-doped  $\text{Ca}_2\text{SiO}_4:\text{Eu}^{2+}$  phosphors have been investigated. Comparing with the  $\text{Ca}_2\text{SiO}_4:\text{Eu}^{2+}$  phosphor, it is found that red-shift of the absorption spectra appears for the Mn-doped  $\text{Ca}_2\text{SiO}_4:\text{Eu}^{2+}$  phosphors. The reason is that  $\text{Mn}^{2+}$  ions substitution on  $\text{Ca}^{2+}$  sites causes an increase of the crystal field strength. Besides, Mn 3d partly enters into the top of the conduction band and the bottom of the valence band. These two reasons bring about narrow band gap and red shift of absorption spectra.

## 锰掺杂对 $\text{Ca}_2\text{SiO}_4:\text{Eu}^{2+}$ 电子结构和光谱性能的影响

陈海涛<sup>1,2</sup>, 黄雪飞<sup>1</sup>, 黄维刚<sup>1</sup>

(1. 四川大学, 四川 成都 610064)

(2. 成都师范学院, 四川 成都 611130)

**摘要:** 运用第一性原理研究了Mn掺杂对 $\text{Ca}_2\text{SiO}_4:\text{Eu}^{2+}$ 荧光粉性能的影响。与 $\text{Ca}_2\text{SiO}_4:\text{Eu}^{2+}$ 荧光粉相比较,发现:进行Mn掺杂以后,荧光粉的吸收光谱向长波方向发生红移。用来替换部分Ca离子的Mn离子提高了 $\text{Eu}^{2+}$ 周围晶体场的强度,造成 $\text{Eu}^{2+}$ 的5d能级的下移。再加上Mn3d能级也发生分裂并部分进入导带顶和价带底,导致带隙变窄和吸收光谱的红移。

**关键词:** 硅酸盐荧光粉; 发光二极管; 第一性原理

作者简介: 陈海涛, 男, 1967年生, 博士, 教授, 四川大学材料科学与工程学院, 四川 成都 610064, 电话: 028-66775489, E-mail:

chqcht@sina.com

**Acknowledgements:** The authors are thankful for the software support by the State Key Laboratory of Polymer materials Engineering of Sichuan University.

### References

- 1 Yonesaki Y, Takei T, Kumada N et al. *Journal of Solid State Chemistry*[J], 2009, 182: 547
- 2 Park C H, Kim T H, Yonesaki Y et al. *Journal of Solid State Chemistry*[J], 2011, 184: 1566
- 3 Choi S, Hong S, Kim Y J et al. *Journal of the American Ceramic Society*[J], 2009, 92: 2025
- 4 Wang B L, Sun L Zh, Ju H D et al. *Materials Letters*[J], 2009, 63: 1329
- 5 Choi N S, Park K W, Park B W et al. *Journal of Luminescence*[J], 2010, 130: 560
- 6 Park K, Choi N, Kim J et al. *Solid State Communications*[J], 2010, 150: 329
- 7 Lee K H, Choi S, Jung H K et al. *Acta Materialia*[J], 2012, 60: 5783
- 8 Yang W J, Chen T M. *Appl Phys Lett*[J], 2006, 88: 101 903
- 9 Li S, Ahuja R. *J Appl Phys*[J], 2005, 97: 103 711
- 10 Bentmann H, Demkov A A, Gregory R et al. *Phys Rev B*[J] 2008, 78: 205 302
- 11 Giacomazzi L, Umari P. *Phys Rev B*[J], 2009, 80: 144 201
- 12 Xu X, Cai C, Hao L Y et al. *Mater Chem Phys*[J], 2009, 118: 270
- 13 Lei T M, Wu S B, Zhang Y M et al. *Rare Metal Materials and Engineering* [J], 2013, 42(12): 2477 (in Chinese)
- 14 Ruan X X, Zhang F C, Zhang W H. *Rare Metal Materials and Engineering*[J], 2015, 44(12): 3027 (in Chinese)
- 15 Milman V, Winkler B, White J A et al. *International Journal of Quantum Chemistry*[J], 2000, 77: 895
- 16 Monkhorst H J, Pack J D. *Physical Review B*[J], 1976, 13: 5188
- 17 Choi S, Hong S, Kiml Y. *J Am Ceram Soc*[J], 2009, 92: 2025
- 18 Mori K, Kiyonagi R, Yonemura M et al. *J Solid State Chem*[J], 2006, 179: 3286